



ORIGINAL RESEARCH

Trace elements-based Auroshell gold@hematite nanostructure: Green synthesis and their hyperthermia therapy

Hadil M. Alahdal¹ | Sumya Ayad Abdullrezzaq² | Hawraz Ibrahim M. Amin^{3,4} |
 Sitah F. Alanazi⁵ | Abduladheem Turki Jalil⁶  | Mehrdad Khatami⁷  |
 Marwan Mahmood Saleh^{8,9}

¹Department of Biology, College of Science, Princess Nourah bint Abdulrahman University, Riyadh, Saudi Arabia

²Medical Laboratory Techniques Department, Al-Maarif University College, Beirut, Iraq

³Department of Chemistry, College of Science, Salahaddin University-Erbil, Erbil, Iraq

⁴Department of Medical Biochemical Analysis, Cihan University-Erbil, Erbil, Iraq

⁵Department of Physics, College of Science, Imam Mohammad Ibn Saud Islamic University, Riyadh, Saudi Arabia

⁶Department of Medical Laboratories Techniques, Al-Mustaqbal University College, Babylon, Hilla, Iraq

⁷Antibacterial Materials R&D Centre, China Metal New Materials (Huzhou) Institute, Huzhou, Zhejiang, China

⁸Department of Biophysics, College of Applied Sciences, University of Anbar, Ramadi, Iraq

⁹Medical Laboratory Technology Department, College of Medical Technology, The Islamic University, Najaf, Iraq

Correspondence

Mehrdad Khatami, Antibacterial Materials R&D Centre, China Metal New Materials (Huzhou) Institute, Huzhou, Zhejiang, China.
 Email: mehrdad7khatami@gmail.com

Abduladheem Turki Jalil, Al-Mustaqbal University College, Babylon, Hilla, 51001, Iraq.
 Email: abedalazcem799@gmail.com

Funding information

Princess Nourah Bint Abdulrahman University, Grant/Award Number: PNURSP2022R150

Abstract

Hyperthermia is an additional treatment method to radiation therapy/chemotherapy, which increases the survival rate of patients without side effects. Nowadays, Auroshell nanoparticles have attracted much attention due to their precise control over heat use for medical purposes. In this research, iron/gold Auroshell nanoparticles were synthesised using green nanotechnology approach. Auroshell gold@hematite nanoparticles were synthesised and characterised with rosemary extract in one step and the green synthesised nanoparticles were characterised by X-ray powder diffraction, SEM, high-resolution transmission electron microscopy, and X-ray photoelectron spectroscopy analysis. Cytotoxicity of Auroshell iron@gold nanoparticles against normal HUVEC cells and glioblastoma cancer cells was evaluated by 2,5-diphenyl-2H-tetrazolium bromide method, water bath hyperthermia, and combined method of water bath hyperthermia and nanotherapy. Auroshell gold@hematite nanoparticles with minimal toxicity are safe against normal cells. The gold shell around the magnetic core of magnetite caused the environmental and cellular biocompatibility of these Auroshell nanoparticles. These magnetic nanoparticles with targeted control and transfer to the tumour tissue led to uniform heating of malignant tumours as the most efficient therapeutic agent.

KEYWORDS

Auroshell nanoparticles, cancer cells, core-shell, core/shell, green chemistry, hyperthermia

1 | INTRODUCTION

Nanostructures refer to particles or structures that have at least one dimension between 1 and 100 nm [1]. A wide range

of compounds/materials, including metals/metals oxide [2] and ceramics [3], such as magnetic [4], silver [5], copper [6], graphene [7], carbon [8], zirconium dioxide [9] and zinc oxide [10] have been synthesised in nanoscale [11] which have wide

This is an open access article under the terms of the Creative Commons Attribution-NonCommercial-NoDerivs License, which permits use and distribution in any medium, provided the original work is properly cited, the use is non-commercial and no modifications or adaptations are made.

© 2022 The Authors. *IET Nanobiotechnology* published by John Wiley & Sons Ltd on behalf of The Institution of Engineering and Technology.

range of medical [12], sanitation [13], catalyst [14], energy [15], sensing [16] and drug delivery [17] applications [18]. Nickel [19], gold [20], aluminium [21], silver [22], titanium [23], iron [24], copper [25] and zinc oxide are the most commonly synthesised nanoparticle [26], and discover synthesis methods for the production of other types [27] of nanoparticles, such as doped [28], hybrid [29], nanofluid [30] and core/shell [31] are necessary [32]. Nanostructures with a dielectric core and a gold shell that can adjust light are called Auroshell [33]. Auroshell cores, known as nanoshells have attracted much attention in diagnostic and cancer therapy. Gold [34] and iron [35] nanoparticles [36] with wide range of applications [37] have received attention in Moore's hyperthermia due to their optical, thermal, and magnetic resonance properties [38]. Auroshell nanostructures penetrate tumours through blood circulation, and after about 24 h of accumulation and effect, they are eliminated from the body through the liver and spleen [39]. In a clinical trial [40], targeted heat therapy of breast cancer cells through blood vessels by antibody-conjugated Auroshells was effective. In this research, the infrared laser causes an increase in the temperature of the gold shell and, as a result, causes the necrosis of cancer cells. Photothermal therapy using fibre optic laser and Auroshell modified with Polyethylene glycol (PEG) caused necrosis of cancer cells. Targeted entry of Auroshell into tumours with PEG-thiol agent resulted in the survival of normal cells [41]. In the clinical trials of gold-silica Auroshells, there was no toxicity on any of the body's organs in the long term [39].

Cancer [42] is the one of the leading causes of death in the world [43]. The cancer burden [44] has grown over time in developing countries [45] due to burgeoning population [46] and ageing [47], accelerating [48]. The U87 glioblastoma cancer cells originate from glial cells, the most common untreated brain tumour in adults. Glioblastoma is the most aggressive malignant tumour with a high rate of growth and spread. Glioblastoma multiforme tumours grow and spread only in the brain, spinal cord, or central nervous system [49]. Glioma cancer cells are fed with abnormal blood vessels abundantly. As a result, the main challenge in treating this cancer is high drug resistance [50], extensive side effects [51], damage to healthy cells [52], high cost of treatment [53], and non-entry of drug macromolecules into the brain due to the blood-brain barrier. Current treatments relieve the disease's symptoms and increase the sufferers' life expectancy up to 15 months. As a result, efficient new treatments and small-scale pharmaceutical molecules are essential for patients' survival [54] and reducing treatment costs [55]. Nowadays, nanomedicines, nanomaterials containing secondary metabolites, antiangiogenic drugs [56], and hyperthermia have attracted much attention [57]. Hyperthermia or heat therapy is one of the complementary methods of cancer treatment in which body tissue is exposed to high heat up to about 113°F. External hyperthermia is applying heat using tools outside the body, such as microwave, ultrasonic, hot water bath, hot water circulation in heating pads, radio frequency etc. The accuracy and depth of heat penetration in external

hyperthermia on the target tissue are low. Applying heat using an external agent inside the body is called internal hyperthermia. The operation area of clinical hyperthermia is divided into three groups: local (target tumour), regional (part of tissue or organ), and global (whole body). Lack of heat distribution in all target cells and heat treatment of healthy cells is a challenge in most heat therapy methods, even regional and local hyperthermia methods. Therefore, researchers turned to nanoscale particles [58], such as gold, iron etc., as heat-sensitive agents [59].

Therefore, the aim of this study was green synthesis of Auroshell nanoparticles using plant extract. Finally, Auroshell toxicity against glioblastoma cancer cells was measured at three temperatures of 41, 43, and 45°C using the external hyperthermia method.

2 | MATERIALS AND METHODS

2.1 | Synthesis of Auroshell gold@hematite nanoparticles

Healthy and young rosemary leaves were disinfected in sodium chlorate (2%) for 1 min and washed several times with deionised water. Then it was dried at room temperature. Healthy rosemary leaves were heated in deionised water for 1 h at 82°C with a ratio of 1:5. The resulting extract was separated with a Buchner funnel. To synthesise gold@hematite core-shell nanoparticles, stock solution of 0.1 M for Iron (III) chloride hexahydrate (97%, Sigma-Aldrich) and Gold (III) chloride trihydrate ($\geq 99.9\%$, Sigma-Aldrich) was added in rosemary extract with a ratio 2:2:1 (Fe: Au: extract) respectively. The final mixture was allowed to stand for 96 h. The gained nanoparticles were washed with deionised water and dried in an oven at 65°C for 999 min.

2.2 | Characterisation of Auroshell gold@hematite nanoparticles

Crystal structures of Auroshell hematite@gold nanoparticles were studied by X-ray powder diffraction analysis (XRD) using X'PertPro, Panalytical Company. XRD analysis was performed with the copper material anode at 2θ from 10° to 80° degree and voltage 40 kV. Field emission scanning electron microscopy (FEI Sigma V.P., ZEISS) equipped with EDS detector and high-resolution transmission electron microscopy (Tecnai Devices. 20) analyses was used to observe the shape, size, and composition of *Auroshell gold@hematite nanoparticles*. Fourier transform infrared spectroscopy (FTIR) of nanoparticles to identify surface functional groups at wavelengths 300–4000 cm^{-1} was performed by using the TENSOR II device, Bruker Company. X-ray photoelectron spectroscopy (XPS) was performed to identify elements and impurities on the surface of nanoparticles by K-Alpha device, Thermofisher Scientific, U.S.

2.3 | Cell culture and cytotoxicity of Auroshell gold@hematite nanoparticles

Human glioblastoma cells (U87) and umbilical vein endothelial cells (HUVEC) were prepared from Pasteur Institute, Tehran, Iran. U87 and HUVEC cells were cultured in Dulbecco's Modified Eagle's Medium (GIBCO) containing glucose, 10% fetal bovine serum (GIBCO), and 10% penicillin/streptomycin (GIBCO) at 37°C, 95% humidity, and 5% carbon dioxide. 2,5-diphenyl-2H-tetrazolium bromide (MTT) test was used to investigate the cell growth inhibition effect of Auroshell gold@hematite nanoparticles. The U87 and HUVEC cells were cultured separately in a 96-well plate with the mentioned conditions for 24 h (Cells were seeded at 2×10^4 cells per well). Then the culture medium was removed, and the cells were treated with concentrations of 5, 10, 20, 40, 60, 80, 100, 250, 500, and 1000 $\mu\text{g/ml}$ Auroshell nanoparticles for 72 h. Then 5 mg/ml of MTT solution (3-(4, 5-Dimethylthiazol-2-yl)-2, 5-diphenyltetrazolium bromide, Sigma-Aldrich) was added to each well and incubated for 4 h. Finally, 100 μl of DMSO solution (dimethyl sulfoxide, Sigma-Aldrich) was added to dissolve formazan crystals, and their optical absorption at 490 nm was read by an ELISA reader (BioTeks Elx 800). Each experiment was repeated three times. Half maximum inhibitory concentration (IC_{50}) was evaluated using the probit test.

2.4 | Combined effect of hyperthermia and nano-therapy on cancer cells

External hyperthermia using a hot water bath was applied on U87 glioblastoma cancer cells in in vitro condition. Cancer cells were cultured in the mentioned conditions to investigate the effects of *Auroshell gold@hematite nanoparticles* and hyperthermia, then treated with concentrations of 5, 10, 20, 40, 60, 80, 100, 250, 500 and 1000 $\mu\text{g/ml}$ Auroshell nanoparticles for 24 h. They were treated and finally immersed in a hot water bath at 41°C for 10 min and 43°C for 30, 45, and 60 min. Also, to investigate the effect of hyperthermia alone, cancer cells

were cultured under the mentioned conditions. Finally, cultures were incubated for 24, 48, and 72 h, and their viability was evaluated by the MTT method [49].

3 | RESULTS AND DISCUSSION

3.1 | Characterisation of Auroshell gold@hematite nanoparticles

Figure 1 shows the XRD spectrum of the Auroshell gold@hematite nanoparticles. Planes (111), (200), (220), and (311) correspond to 2θ peaks of 38, 44, 64, and 78°, respectively, of the face-centred cubic phase of gold nanoparticles [60]. The average size of nanoparticle crystallite with the Debye-Scherrer formula and based on the sharpest peak ($2\theta = 38.320$) is 25.65 nm.

$$D = \frac{K\lambda}{\beta \cos\theta} \quad (1)$$

In the above formula (Equation 1), ' k ' is the crystal shape coefficient and ' λ ': X-ray wavelength. The XRD graph has no additional peaks, so the synthesised nanoparticles are pure and crystalline. Also, due to the presence of gold shells on the surface of the heavy ionic nature of iron, there is no peak of iron particles in the graph. According to the literature, the reactivity speed of iron precursors with phenolic extract is very high, so by adding iron stock to rosemary extract, black iron nanoparticles are immediately formed [8].

The XPS spectrum of Auroshell gold@hematite nanoparticles in Figure 2a confirmed the presence of Fe2p, Au4f, C1s, and O1s elements. Figure 2b shows two significant peaks and 10 satellite peaks for iron. The satellite peaks of 708.8 eV and 712.57 correspond to Fe^{2+} and Fe^{3+} ions respectively. Fe2p1 and Fe2p3 peaks at 723.96 and 710.36 eV are the zero-iron states, confirming gold shells. The existence of different ionic states of iron is caused by the thin coating of gold (<4 nm) and the oxidation of iron. It is also due to the intense peaks of iron (iii) ion of Fe_3O_4 nanoparticle core.

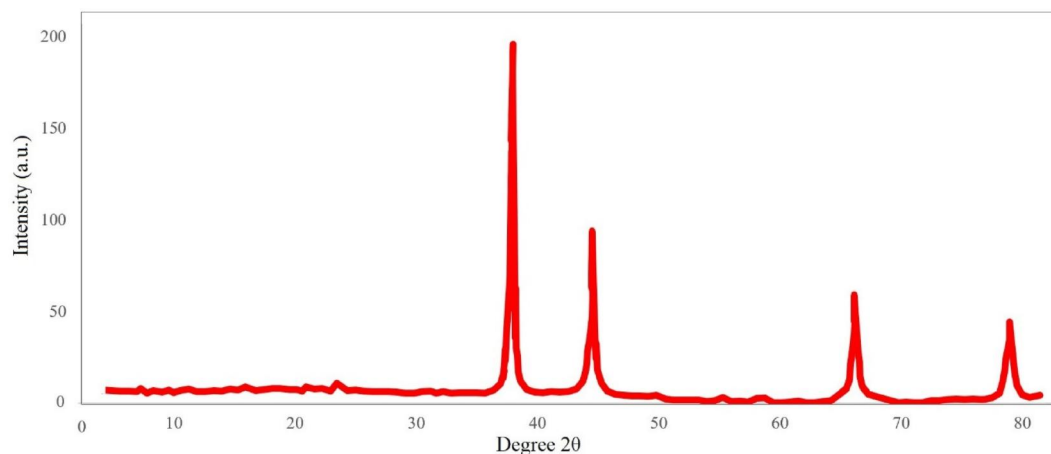


FIGURE 1 X-ray powder diffraction pattern of Auroshell gold@hematite nanoparticles.

Au4f peaks at 84 and 88 eV show that the gold particles are like a coating around the iron particles. In Figure 2c, oxygen satellite peaks in the energy band of 532.62 and 530.41 eV confirm the Auroshell gold@hematite structure. Also, the central peak of oxygen in the energy band of 531.48 electron volts corresponds to the structure of Fe_3O_4 . The presence of C1s peaks corresponds to organic substances in rosemary extract. The central peak of carbon in the energy band of 284.65 electron volts corresponds to the alkyl group of rosemary extract.

The FESEM image of Auroshell gold@hematite nanoparticles shows spherical and ellipsoidal particles at a 100Kx scale (Figure 3a). Figure 3b shows the Energy-dispersive X-ray spectroscopy micrograph of Auroshell gold@hematite nanoparticles. Auroshell gold@hematite nanoparticles have elements of gold, carbon, oxygen, iron, and chlorine with weight percentages of 7.96, 33.09, 43.33, 11.23, and 4.38 wt%

respectively. Carbon and chlorine in the structure of Auroshell gold@hematite nanoparticles correspond to plant extract and iron precursor respectively.

Figure 4 shows the HRTEM image of Auroshell gold@hematite nanoparticles at a scale of 50 nm with a bright background. Dark central and surface grey regions correspond to the iron core and gold shell nanoparticles [61]. As seen in the picture, the thickness of the shell varies throughout the particles; even in some areas, it is <4 nm. This thickness is consistent with the XPS data. The variable thickness of the Auroshell shell has caused the creation of nanoparticles with uneven surfaces.

Figure 5 shows the FTIR spectra of rosemary extract (Figure 5a) and Auroshell gold@hematite nanoparticles (Figure 5b). The broad spectra of rosemary extract in the 3448.9, 1637.72, and 606 to 521 cm^{-1} respectively correspond to the hydroxyl group of phenolic compounds, carboxyl group, and C-H group. Also, the spectrum observed in region 2092 of

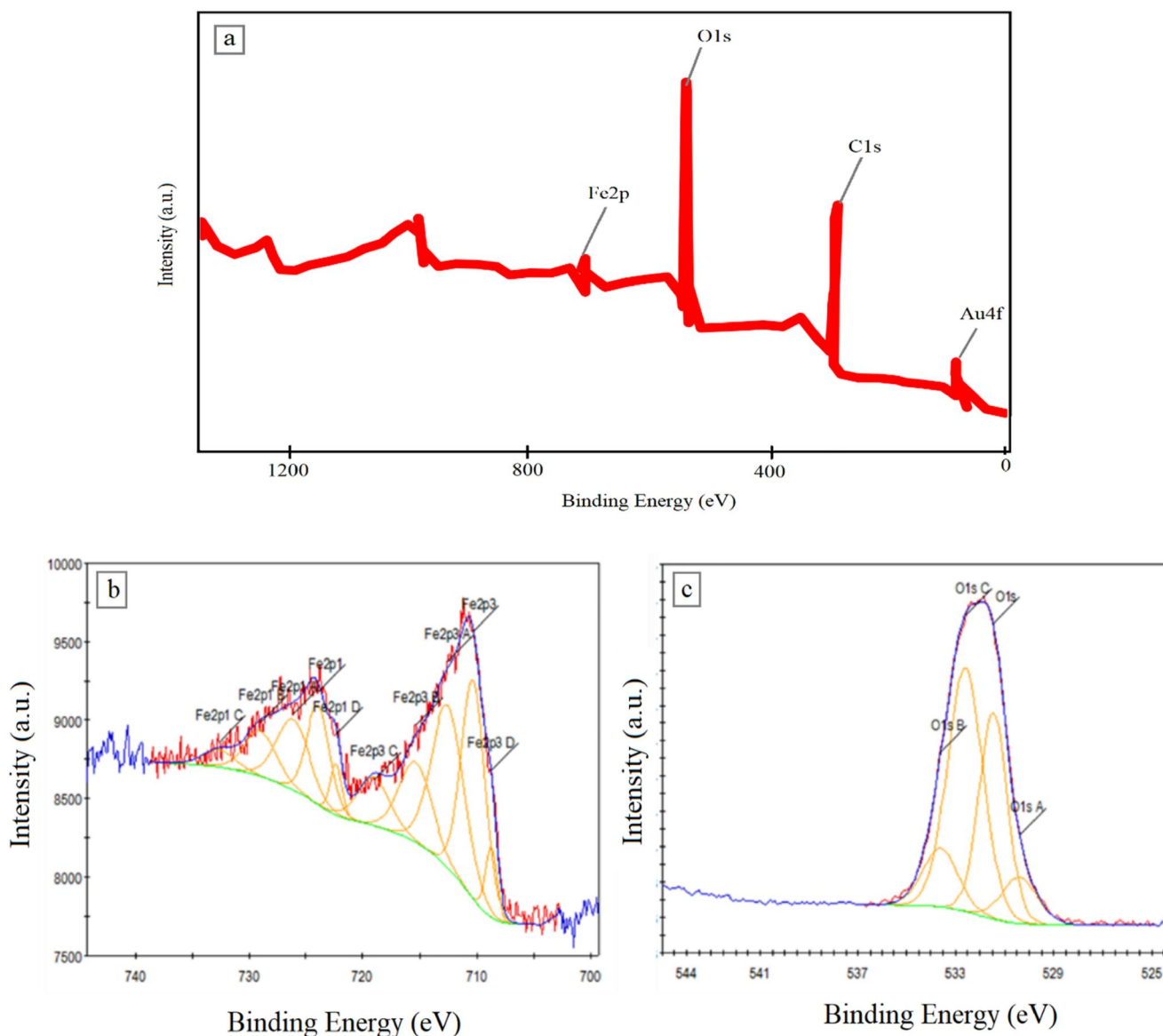


FIGURE 2 X-ray photoelectron spectroscopy pattern of Auroshell gold@hematite nanoparticles (a) Fe2p region (b) and O1s electron XPS spectra (c).

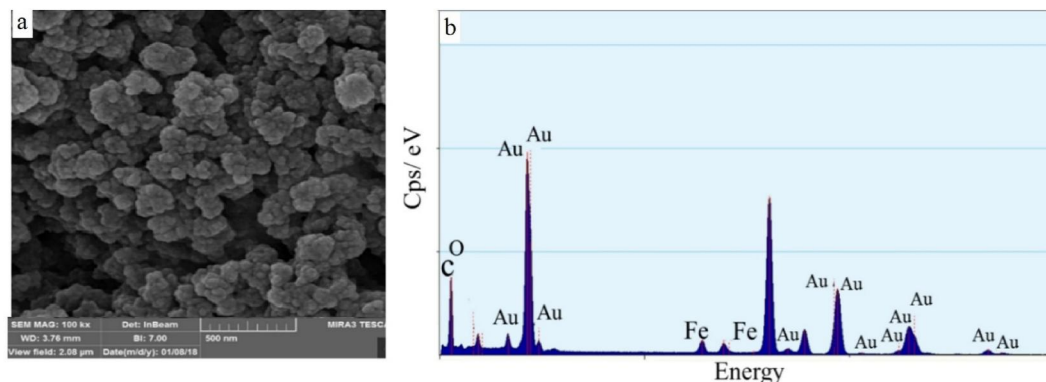


FIGURE 3 FE-SEM micrographs and (a) Energy-dispersive X-ray spectroscopy spectrum of Auroshell gold@hematite nanoparticles (b). FE-SEM, field emission-scanning electron microscopy.

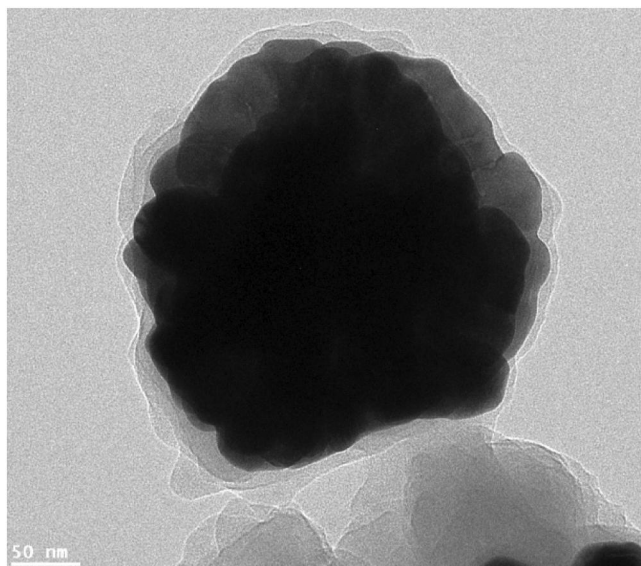


FIGURE 4 High-resolution transmission electron microscopy micrograph of Auroshell gold@hematite nanoparticles.

rosemary extract corresponds to the alkyl group of rosmarinic acid. The broad peak of 3449 cm^{-1} in the spectrum of Auroshell gold@hematite nanoparticles confirms the reducing role of the hydroxyl group of phenols in the extract. Peaks in the region of 2073 and 1637 cm^{-1} of nanoparticles confirm the vibrational bonds of alkyl and carboxyl groups in the core-shell particles respectively. Also, the peaks of the 607 to 487 spectrums of Auroshell nanoparticles show the iron-oxygen bond in the iron oxide core.

3.2 | Cell viability assay of Auroshell gold@hematite nanoparticles

Cell viability assay of biogenic Auroshell gold@hematite nanoparticles on U87 cancer cells was evaluated by the MTT method for 24, 48, and 72 h (Figure 6). The results show that the CC_{50} value of biogenic nanoparticles against normal cells is $347.8\text{ }\mu\text{g/ml}$ and the IC_{50} value of Auroshell

gold@hematite nanoparticles on the glioblastoma cancer cell line is $51.8\text{ }\mu\text{g/ml}$. Half of the cancer cells in the concentration of $50\text{ }\mu\text{g/ml}$ Auroshell gold@hematite nanoparticles have suffered cell wall rupture and apoptosis. The survival of the studied cells has an inverse relationship with the concentration of their nanoparticles.

3.3 | Combined effect of hyperthermia and nano-therapy

The results show the combined effect of nano-therapy and hyperthermia. The highest mortality rate is at 45°C and in 60 min. By increasing the temperature and duration of the water bath, the lowest nanoparticle concentration has caused the maximum death of cancer cells. The survival of cancer cells in the glioblastoma water bath method has been higher than in the other two methods. Because, unlike normal body cells, cancer cells can grow and multiply at high temperatures [62]. The nano-size of nanoparticles provides the possibility of passing through the cell wall and increasing the temperature in the deep areas of the tumour tissue [63]. Gold nanoparticles are more interested in infrared hyperthermia due to their unique optical properties. Chen et al [63] proved in their studies that rod gold nanoparticles with uneven surfaces are ineffective in hyperthermia caused by radio waves. These nanoparticles cannot spread heat. Also, gold hyperthermia in the extracellular region was unsuccessful. Hyperthermia of mammary adenocarcinoma cells (M TG-B) cells delayed the proliferation of cells in this vivo condition by magnetic iron nanoparticles. Also, the percentage of death of MTG-B cancer cells in iron nanoparticle water bath hyperthermia at 35°C was higher than in water bath hyperthermia alone. This is due to iron nanoparticles' ability to increase heat [62]. Magnetic hyperthermia and water bath of breast cancer cells were evaluated at 41, 45, and 50°C with iron nanoparticles. The results showed that hyperthermia of MCF-7 cells was more effective at a temperature of 50°C , so the survival of cancer cells at this temperature was negligible. Also, this research showed that iron magnetic hyperthermia is not more efficient than iron water bath hyperthermia. The efficiency of nanoparticle

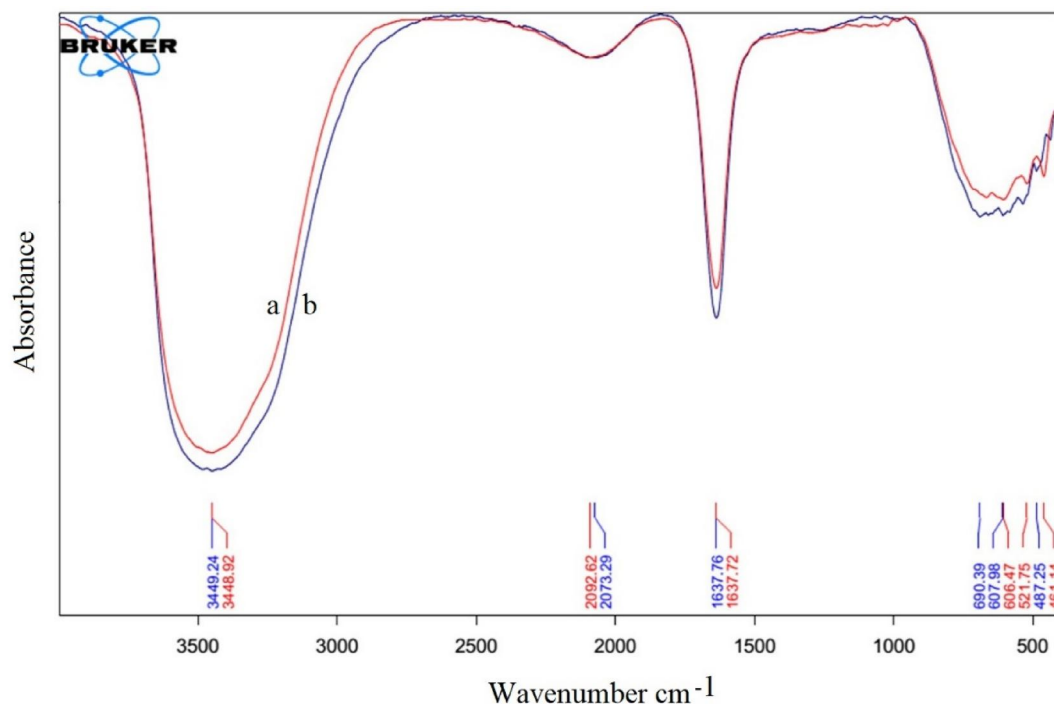


FIGURE 5 Fourier transform infrared spectroscopy spectra of Rosemary extract (a) and Auroshell gold@hematite nanoparticles (b).

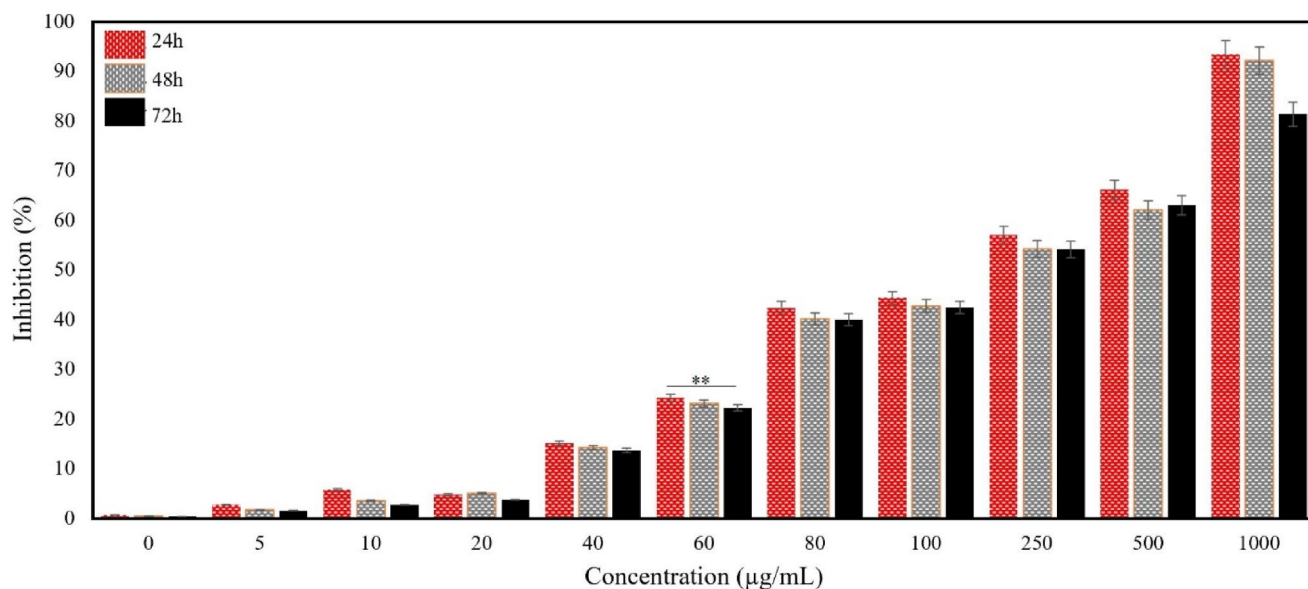


FIGURE 6 Cytotoxicity of Auroshell gold@hematite nanoparticles on U87 cancer cells for 24 (red columns), 48 (grey columns) and 72 (black columns) hours. (** $p < 0.05$ compared with untreated cells).

hyperthermia depends on the hyperthermia temperature, type, concentration, shape and size of nanoparticles, time and cytotoxicity measurement method [64].

4 | CONCLUSION

In this research, Auroshell gold@hematite nanoparticles were synthesised and characterised with rosemary extract in one

step. Auroshell gold@hematite nanoparticles have minimal toxicity against normal cells. The gold shell around the magnetic core of magnetite caused the environmental and cellular biocompatibility of these Auroshell nanoparticles. The multi-functional use of Auroshell nanoparticles has attracted much attention in the adjunctive treatment of hyperthermia. Therefore, we evaluated the potential of biogenic synthesised nanoparticles in vitro against *Globostoma* cancer cells by the water bath hyperthermia method. According to the results, the

duration of treatment and the amount of temperature applied with the dose of Auroshell gold@hematite nanoparticles have a synergistic effect. So, the survival of cancer cells in the concentration of about 1000 $\mu\text{g/ml}$ of nanoparticles at 45°C for 60 min reached almost zero. The magnetic nature of the magnetite core enables the targeted delivery of synthesis nanoparticles to cancer tumours. Also, the nanometre size of synthetic nanoparticles provides passage through the blood–brain barrier through blood circulation. As a result, side effects of treatment and damage to healthy tissues are minimised. It is suggested that magnetic hyperthermia and photothermal therapy of green synthesis iron@gold nanoparticles can be evaluated in vivo to treat glioblastoma.

AUTHOR CONTRIBUTIONS

All the authors contributed to the design, data acquisition, analysis, interpretation and presentation of this work. The corresponding author is responsible for the author contributions. All the authors have read and approved the final manuscript.

ACKNOWLEDGEMENT

This work was funded by the Princess Nourah bint Abdulrahman University Researchers Supporting Project number (PNURSP2022R150), Princess Nourah bint Abdulrahman University, Riyadh, Saudi Arabia.

CONFLICT OF INTEREST

The authors confirm that the content of this article involves no competing interests.

DATA AVAILABILITY STATEMENT

The data that support the findings of this study are available from corresponding author.

ORCID

Abdulbeem Turki Jalil  <https://orcid.org/0000-0001-8403-7465>

Mehrdad Khatami  <https://orcid.org/0000-0002-7519-6998>

REFERENCES

1. a) Ameen, F., et al.: Flavonoid dihydromyricetin-mediated silver nanoparticles as potential nanomedicine for biomedical treatment of infections caused by opportunistic fungal pathogens. *Res. Chem. Intermed.* 44(9), 5063–5073 (2018). <https://doi.org/10.1007/s11164-018-3409-x> b) Chupradit, S., et al.: Use of organic and copper-based nanoparticles on the turbulator instalment in a shell tube heat exchanger: a CFD-based simulation approach by using nanofluids. *J. Nanomater.* 2021, 1–7 (2021). <https://doi.org/10.1155/2021/3250058>
2. a) Akbarizadeh, M.R., et al.: Thematic issue: hydrothermal conversion of biomass. *Biomass Convers. Biorefin.* 12, 1–12 (2022). <https://doi.org/10.1007/s13399-021-01927-7> b) Khatami, M., et al.: Simplification of gold nanoparticle synthesis with low cytotoxicity using a greener approach: opening up new possibilities. *RSC Adv.* 11(6), 3288–3294 (2021). <https://doi.org/10.1039/d0ra08822f> c) Xin Cui, C.L., et al.: Cryogenic minimum quantity lubrication machining: from mechanism to application. *Front. Mech. Eng.* 16(4), 649–697 (2021). <https://doi.org/10.1007/s11465-021-0654-2>
3. a) Yang, M., et al.: Maximum undeformed equivalent chip thickness for ductile–brittle transition of zirconia ceramics under different lubrication conditions. *Int. J. Mach. Tool Manufact.* 122, 55–65 (2017). <https://doi.org/10.1016/j.ijmactools.2017.06.003> b) Yang, M., et al.: Research on microscale skull grinding temperature field under different cooling conditions. *Appl. Therm. Eng.* 126, 525–537 (2017). <https://doi.org/10.1016/j.applthermaleng.2017.07.183>
4. a) Moghadam, N.C.Z., et al.: Nickel oxide nanoparticles synthesis using plant extract and evaluation of their antibacterial effects on *Streptococcus mutans*. *Bioproc. Biosyst. Eng.* 45(7), 1201–1210 (2022). <https://doi.org/10.1007/s00449-022-02736-6> b) He, X., et al.: MgFe-LDH nanoparticles: a promising leukemia inhibitory factor replacement for self-renewal and pluripotency maintenance in cultured mouse embryonic stem cells. *Adv. Sci.* 8(9), 2003535 (2021). <https://doi.org/10.1002/adv.202003535>
5. a) Almansob, A., et al.: Effective treatment of resistant opportunistic fungi associated with immuno-compromised individuals using silver biosynthesized nanoparticles. *Appl. Nanosci.* 1–12 (2022) b) Begum, I., et al.: A combinatorial approach towards antibacterial and antioxidant activity using tartaric acid capped silver nanoparticles. *Processes.* 10(4), 716 (2022). <https://doi.org/10.3390/pr10040716>
6. Ameen, F.: Optimization of the synthesis of fungus-mediated Bi-metallic Ag-Cu nanoparticles. *Appl. Sci.* 12(3), 1384 (2022). <https://doi.org/10.3390/app12031384>
7. Khan, A., et al.: Fabrication and antibacterial activity of nanoenhanced conjugate of silver (I) oxide with graphene oxide. *Mater. Today Commun.* 25, 101667 (2020). <https://doi.org/10.1016/j.mtcomm.2020.101667>
8. Ngafwan, N., et al.: Study on novel fluorescent carbon nanomaterials in food analysis. *Food Sci. Technol.* 42 (2021). <https://doi.org/10.1590/fst.37821>
9. Isacfranklin, M., et al.: Synthesis of highly active biocompatible ZrO₂ nanorods using a bioextract. *Ceram. Int.* 46(16), 25915–25920 (2020). <https://doi.org/10.1016/j.ceramint.2020.07.076>
10. a) Indhira, D., et al.: Biomimetic facile synthesis of zinc oxide and copper oxide nanoparticles from *Elaeagnus indica* for enhanced photocatalytic activity. *Environ. Res.* 212, 113323 (2022). <https://doi.org/10.1016/j.envres.2022.113323> b) Ameen, F., Dawoud, T., AlNadhari, S.: Ecofriendly and low-cost synthesis of ZnO nanoparticles from *Acremonium potronii* for the photocatalytic degradation of azo dyes. *Environ. Res.* 202, 111700 (2021). <https://doi.org/10.1016/j.envres.2021.111700>
11. AlNadhari, S., et al.: A review on biogenic synthesis of metal nanoparticles using marine algae and its applications. *Environ. Res.* 194, 110672 (2021). <https://doi.org/10.1016/j.envres.2020.110672>
12. a) Subramaniyan, S.B., et al.: Phytolectin-cationic lipid complex revive ciprofloxacin efficacy against multi-drug resistant uropathogenic *Escherichia coli*. *Colloids Surf. A Physicochem. Eng. Asp.* 647, 128970 (2022). <https://doi.org/10.1016/j.colsurfa.2022.128970> b) Mohammed, A.E., et al.: In-silico predicting as a tool to develop plant-based biomedicines and nanoparticles: *Lycium shawii* metabolites. *Biomed. Pharmacother.* 150, 113008 (2022). <https://doi.org/10.1016/j.biopha.2022.113008> c) Gangalla, R., et al.: Optimization and characterisation of exopolysaccharide produced by *Bacillus aerophilus* rk1 and its in vitro antioxidant activities. *J. King Saud Univ. Sci.* 33(5), 101470 (2021). <https://doi.org/10.1016/j.jksus.2021.101470> d) Sarika, K., et al.: Antimicrobial and antifungal activity of soil actinomycetes isolated from coal mine sites. *Saudi J. Biol. Sci.* 28(6), 3553–3558 (2021). <https://doi.org/10.1016/j.sjbs.2021.03.029> e) Yang, Y., et al.: Machinability of ultrasonic vibration assisted micro-grinding in biological bone using nanolubricant. *Front. Mech. Eng.* 22(17), 1–8 (2022)
13. a) Selvam, K., et al.: Laccase production from *Bacillus aestuarii* KSK using *Borassus flabellifer* empty fruit bunch waste as a substrate and assessing their malachite green dye degradation. *J. Appl. Microbiol.* (2022). <https://doi.org/10.1111/jam.15670> b) Alshehrei, F., Al-Enazi, N. M., Ameen, F.: Biomass Convers. Biorefin., 1–8 (2021) c) Mostafa, A.A.-F., et al.: In vitro evaluation of antifungal activity of some agricultural fungicides against two saprolegnoid fungi infecting cultured fish. *J. King Saud Univ. Sci.* 32(7), 3091–3096 (2020). <https://doi.org/10.1016/j.jksus.2020.08.019> d) Ali, M., et al.: An environmentally friendly solution for waste facial masks recycled in construction materials. Sustainability

- 14, 8739 (2022). <https://doi.org/10.3390/su14148739> e) Kartika, R., et al.: Ca12O12 nanocluster as highly sensitive material for the detection of hazardous mustard gas: density-functional theory. *Inorg. Chem. Commun.* 137, 109174 (2022). <https://doi.org/10.1016/j.inoche.2021.109174>
14. a) Sadeghi, M., et al.: Dichlorosilane adsorption on the Al, Ga, and Zn-doped fullerenes. *Monatsh. Chem.*, 1–8 (2022) b) Khatami, M., Irvani, S.: Green and eco-friendly synthesis of nanophotocatalysts: an overview. *Comments Mod. Chem.* 41(3), 133–187 (2021). <https://doi.org/10.1080/02603594.2021.1895127>
15. a) Sivaraman, R., et al.: Evaluating the potential of graphene-like boron nitride as a promising cathode for Mg-ion batteries. *J. Electroanal. Chem.* 917, 116413 (2022). <https://doi.org/10.1016/j.jelechem.2022.116413> b) Anqi, A.E., et al.: Effect of combined air cooling and nano enhanced phase change materials on thermal management of lithium-ion batteries. *J. Energy Storage* 52, 104906 (2022). <https://doi.org/10.1016/j.est.2022.104906>
16. a) Chupradit, S., et al.: Various types of electrochemical biosensors for leukemia detection and therapeutic approaches. *Anal. Biochem.* 114736 (2022) b) Khaki, N., et al.: Sensing of acetaminophen drug using Zn-doped boron nitride nanocones: a DFT inspection. *Appl. Biochem. Biotechnol.* 194(6), 2481–2491 (2022). <https://doi.org/10.1007/s12010-022-03830-x> c) Olegovich Bokov, D., et al.: Ir-decorated gallium nitride nanotubes as a chemical sensor for recognition of mesalamine drug: a DFT study. *Mol. Simulat.* 48(5), 438–447 (2022). <https://doi.org/10.1080/08927022.2021.2025234>
17. a) Lai, W.-F.: Non-conjugated polymers with intrinsic luminescence for drug delivery. *J. Drug Deliv. Sci. Technol.* 59, 101916 (2020). <https://doi.org/10.1016/j.jddst.2020.101916> b) Lai, W.-F., Tang, R., Wong, W.-T.: Ionically crosslinked complex gels loaded with oleic acid-containing vesicles for transdermal drug delivery. *Pharmaceutics* 12(8), 725 (2020). <https://doi.org/10.3390/pharmaceutics12080725> c) Choi, Y., et al.: Students' perception and expectation towards pharmacy education: a qualitative study of pharmacy students in a developing country. *Indian J. Pharmaceut. Educ. Res.* 55(1), 63–69 (2021). <https://doi.org/10.5530/ijper.55.1.9>
18. a) Bokov, D., et al.: Nanomaterial by sol-gel method: synthesis and application. *Adv. Mater. Sci. Eng.* 2021, 1–21 (2021). <https://doi.org/10.1155/2021/5102014> b) Jalil, A.T., et al.: High-sensitivity biosensor based on glass resonance PhC cavities for detection of blood component and glucose concentration in human urine. *Coatings* 11(12), 1555 (2021). <https://doi.org/10.3390/coatings11121555> c) Anzum, R., et al.: A review on separation and detection of copper, cadmium, and chromium in food based on cloud point extraction technology. *Food Sci. Technol.* 42 (2022). <https://doi.org/10.1590/fst.80721> d) Wang, X., et al.: Tribology of enhanced turning using biolubricants: a comparative assessment. *Tribol. Int.* 174, 107766 (2022). <https://doi.org/10.1016/j.triboint.2022.107766>
19. Li, B., et al.: Grinding temperature and energy ratio coefficient in MQL grinding of high-temperature nickel-base alloy by using different vegetable oils as base oil. *Chin. J. Aeronaut.* 29(4), 1084–1095 (2016). <https://doi.org/10.1016/j.cja.2015.10.012>
20. Ameen, F., et al.: Soil bacteria *Cupriavidus* sp. mediates the extracellular synthesis of antibacterial silver nanoparticles. *J. Mol. Struct.* 1202, 127233 (2020). <https://doi.org/10.1016/j.molstruc.2019.127233>
21. a) Duan, Z., et al.: Cryogenic minimum quantity lubrication machining: from mechanism to application. *Front. Mech. Eng.* 16(4), 649–697 (2022). <https://doi.org/10.1007/s11465-021-0654-2> b) Duan, Z., et al.: Milling surface roughness for 7050 aluminum alloy cavity influenced by nozzle position of nanofluid minimum quantity lubrication. *Chin. J. Aeronaut.* 34(6), 33–53 (2021). <https://doi.org/10.1016/j.cja.2020.04.029>
22. a) Valarmathi, N., et al.: Utilization of marine seaweed *Spyridia filamentosa* for silver nanoparticles synthesis and its clinical applications. *Mater. Lett.* 263, 127244 (2020). <https://doi.org/10.1016/j.matlet.2019.127244> b) Ameen, F., et al.: Phytosynthesis of silver nanoparticles using *Mangifera indica* flower extract as bioreductant and their broad-spectrum antibacterial activity. *Bioorg. Chem.* 88, 102970 (2019). <https://doi.org/10.1016/j.bioorg.2019.102970>
23. c) Cui, X., et al.: Grindability of titanium alloy using cryogenic nanolubricant minimum quantity lubrication. *J. Manuf. Process.* 80, 273–286 (2022). <https://doi.org/10.1016/j.jmappro.2022.06.003>
24. a) Akbarizadeh, M.R., et al.: Cytotoxic activity and magnetic behavior of green synthesized iron oxide nanoparticles on brain glioblastoma cells. *Nanomed. Res. J.* 7, 99–106 (2022) b) Sadeghi, H., et al.: Iron oxyhydroxide nanoparticles: green synthesis and their cytotoxicity activity against A549 human lung adenocarcinoma cells. *Rend. Lincei Sci. Fis. Nat.* 33, 461–469 (2022) c) Jasim, S.A., et al.: Green synthesis of spinel copper ferrite (CuFe₂O₄) nanoparticles and their toxicity. *Nanotechnol. Rev.* 11(1), 2483–2492 (2022). <https://doi.org/10.1515/ntrev-2022-0143>
25. a) Naveenraj, S., et al.: A general microwave synthesis of metal (Ni, Cu, Zn) selenide nanoparticles and their competitive interaction with human serum albumin. *New J. Chem.* 42(8), 5759–5766 (2018). <https://doi.org/10.1039/c7nj04316c> b) Ghodake, G.S., et al.: Colorimetric detection of Cu²⁺ based on the formation of peptide–copper complexes on silver nanoparticle surfaces. *Beilstein J. Nanotechnol.* 9, 1414–1422 (2018). <https://doi.org/10.3762/bjnano.9.134>
26. a) Begum, I., et al.: Facile fabrication of malonic acid capped silver nanoparticles and their antibacterial activity. *J. King Saud Univ. Sci.* 33(1), 101231 (2021). <https://doi.org/10.1016/j.jksus.2020.101231> b) Ameen, F., et al.: Fabrication of silver nanoparticles employing the cyanobacterium *Spirulina platensis* and its bactericidal effect against opportunistic nosocomial pathogens of the respiratory tract. *J. Mol. Struct.* 1217, 128392 (2020). <https://doi.org/10.1016/j.molstruc.2020.128392> c) Ahmed, B., et al.: Destruction of cell topography, morphology, membrane, inhibition of respiration, biofilm formation, and bioactive molecule production by nanoparticles of Ag, ZnO, CuO, TiO₂, and Al₂O₃ toward beneficial soil bacteria. *ACS Omega* 5(14), 7861–7876 (2020). <https://doi.org/10.1021/acsomega.9b04084> c) Mythili, R., et al.: Utilization of market vegetable waste for silver nanoparticle synthesis and its antibacterial activity. *Mater. Lett.* 225, 101–104 (2018). <https://doi.org/10.1016/j.matlet.2018.04.111> d) Kim, D.-Y., et al.: Green synthesis of silver nanoparticles using *Laminaria japonica* extract: characterisation and seedling growth assessment. *J. Clean. Prod.* 172, 2910–2918 (2018). <https://doi.org/10.1016/j.jclepro.2017.11.123>
27. Safaei, M., et al.: A review on metal-organic frameworks: synthesis and applications. *TrAC Trends Anal. Chem.* 118, 401–425 (2019). <https://doi.org/10.1016/j.trac.2019.06.007>
28. a) Rao, M.P., et al.: Synthesis of N-doped potassium tantalate perovskite material for environmental applications. *J. Solid State Chem.* 258, 647–655 (2018). <https://doi.org/10.1016/j.jssc.2017.11.031> b) Mortezaagholi, B., et al.: Plant-mediated synthesis of silver-doped zinc oxide nanoparticles and evaluation of their antimicrobial activity against bacteria cause tooth decay. *Microsc. Res. Tech.* 85(11), 3553–3564 (2022). <https://doi.org/10.1002/jemt.24207> c) Cao, Y., et al.: K-doped ZnO nanostructures: biosynthesis and parasitocidal application. *J. Mater. Res. Technol.* 15, 5445–5451 (2021). <https://doi.org/10.1016/j.jmrt.2021.10.137>
29. Mirzaiebadizi, A., et al.: An intelligent DNA nanorobot for detection of MiRNAs cancer biomarkers using molecular programming to fabricate a logic-responsive hybrid nanostructure. *Bioproc. Biosyst. Eng.* 45(11), 1781–1797 (2022). <https://doi.org/10.1007/s00449-022-02785-x>
30. a) Wang, Y., et al.: Processing characteristics of vegetable oil-based nanofluid MQL for grinding different workpiece materials. *Int. J. Precis. Eng. Manuf. Green Technol.* 5(2), 327–339 (2018). <https://doi.org/10.1007/s40684-018-0035-4> b) Zhang, J., et al.: Experimental assessment of an environmentally friendly grinding process using nanofluid minimum quantity lubrication with cryogenic air. *J. Clean. Prod.* 193, 236–248 (2018). <https://doi.org/10.1016/j.jclepro.2018.05.009> c) Tang, L., et al.: Biological stability of water-based cutting fluids: progress and application. *Chin. J. Mech. Eng.* 35(1), 3 (2022). <https://doi.org/10.1186/s10033-021-00667-z>
31. Shafiee, A., et al.: Core-shell nanophotocatalysts: review of materials and applications. *ACS Appl. Nano Mater.* 5(1), 55–86 (2022). <https://doi.org/10.1021/acsnm.1c03714>

32. a) Akbarizadeh, M.R., Sarani, M., Darijani, S.: Study of antibacterial performance of biosynthesised pure and Ag-doped ZnO nanoparticles. *Rend. Lincei Sci. Fis. Nat.* 33(3), 1–9 (2022). <https://doi.org/10.1007/s12210-022-01079-4> b) Arkaban, H., et al.: Polyacrylic acid nanoplatfoms: antimicrobial, tissue engineering, and cancer theranostic applications. *Polymers* 14(6), 1259 (2022). <https://doi.org/10.3390/polym14061259>
33. Benjamin, T.G., et al.: Alternatives to whole gland treatment for localized prostate cancer: a review of novel focal therapies. *Curr. Opin. Urol.* 32(3), 239–247 (2022). <https://doi.org/10.1097/mou.0000000000000981>
34. a) Megarajan, S., et al.: Synthesis of N-myristoyltaurine stabilised gold and silver nanoparticles: assessment of their catalytic activity, antimicrobial effectiveness and toxicity in zebrafish. *Environ. Res.* 212, 113159 (2022). <https://doi.org/10.1016/j.envres.2022.113159> b) Mythili, R., et al.: Biogenic synthesis, characterisation and antibacterial activity of gold nanoparticles synthesised from vegetable waste. *J. Mol. Liq.* 262, 318–321 (2018). <https://doi.org/10.1016/j.molliq.2018.04.087>
35. a) Swathi, S., et al.: Cancer targeting potential of bioinspired chain like magnetite (Fe₃O₄) nanostructures. *Curr. Appl. Phys.* 20(8), 982–987 (2020). <https://doi.org/10.1016/j.cap.2020.06.013> b) AlYahya, S., et al.: Size dependent magnetic and antibacterial properties of solvothermally synthesised cuprous oxide (Cu₂O) nanocubes. *J. Mater. Sci. Mater. Electron.* 29(20), 17622–17629 (2018). <https://doi.org/10.1007/s10854-018-9865-7> c) Hachem, K., et al.: Adsorption of Pb(II) and Cd(II) by magnetic chitosan-salicylaldehyde Schiff base: synthesis, characterisation, thermal study and antibacterial activity. *J. Chin. Chem. Soc.* 69(3), 512–521 (2022). <https://doi.org/10.1002/jccs.202100507>
36. a) Iram, S., et al.: Gold nanoconjugates reinforce the potency of conjugated cisplatin and doxorubicin. *Colloids Surf. B Biointerfaces* 160, 254–264 (2017). <https://doi.org/10.1016/j.colsurfb.2017.09.017> b) Hu, X., et al.: The microchannel type effects on water-Fe₃O₄ nanofluid atomic behavior: molecular dynamics approach. *J. Taiwan Inst. Chem. Eng.* 135, 104396 (2022). <https://doi.org/10.1016/j.jtice.2022.104396>
37. a) Almansob, A., Bahkali, A.H., Ameen, F.: Efficacy of gold nanoparticles against drug-resistant nosocomial fungal pathogens and their extracellular enzymes: resistance profiling towards established antifungal agents. *Nanomaterials* 12(5), 814 (2022). <https://doi.org/10.3390/nano12050814> b) Ameen, F., et al.: Antioxidant, antibacterial and anticancer efficacy of *Alternaria chlamydospora*-mediated gold nanoparticles. *Appl. Nanosci.* 12, 1–8 (2022) c) Alsamhary, K., et al.: Gold nanoparticles synthesised by flavonoid tricetin as a potential antibacterial nanomedicine to treat respiratory infections causing opportunistic bacterial pathogens. *Microb. Pathog.* 139, 103928 (2020). <https://doi.org/10.1016/j.micpath.2019.103928>
38. a) Rahim, M., et al.: Nutratherapeutics approach against cancer: tomato-mediated synthesised gold nanoparticles. *IET Nanobiotechnol.* 12, 1–5 (2018). <https://doi.org/10.1049/iet-nbt.2017.0068> b) Jasni, M.J.F., et al.: Fabrication, characterisation and application of laccase–nylon 6, 6/Fe³⁺ composite nanofibrous membrane for 3, 3'-dimethoxybenzidine detoxification. *Bioproc. Biosyst. Eng.* 40(2), 191–200 (2017). <https://doi.org/10.1007/s00449-016-1686-6>
39. Gad, S.C., et al.: Evaluation of the toxicity of intravenous delivery of Auroshell particles (Gold–Silica nanoshells). *Int. J. Toxicol.* 31(6), 584–594 (2012). <https://doi.org/10.1177/1091581812465969>
40. Aslan, B., et al.: Nanotechnology in cancer therapy. *J. Drug Target.* 21(10), 904–913 (2013). <https://doi.org/10.3109/1061186x.2013.837469>
41. Abadeer, N.S., Murphy, C.J.: Recent progress in cancer thermal therapy using gold nanoparticles. *Nanomater. Neoplasms*, 143–217 (2021)
42. a) Jalil, A.T., et al.: Cancer stages and demographical study of HPV16 in gene L2 isolated from cervical cancer in Dhi-Qar province, Iraq. *Appl. Nanosci.*, 1–7 (2021) b) Sundram, T., Zakaria, M.H.B., Nasir, M.: Anti-oxidant and cytotoxic effects of *Curcuma mangga* and *Bosenbergia rotunda* ethanolic extracts on Mcf-7 cancer cell lines. *Science* 3, 10–14 (2019)
43. a) Kumar, V., et al.: Evaluation of cytotoxicity and genotoxicity effects of refractory pollutants of untreated and biometanated distillery effluent using *Allium cepa*. *Environ. Pollut.* 300, 118975 (2022). <https://doi.org/10.1016/j.envpol.2022.118975> b) Rajadurai, U.M., et al.: Assessment of behavioral changes and antitumor effects of silver nanoparticles synthesised using diosgenin in mice model. *J. Drug Deliv. Sci. Technol.* 66, 102766 (2021). <https://doi.org/10.1016/j.jddst.2021.102766> c) Ameen, F., et al.: Anti-oxidant, anti-fungal and cytotoxic effects of silver nanoparticles synthesised using marine fungus *Cladosporium halotolerans*. *Appl. Nanosci.*, 1–9 (2021)
44. a) Saleh, R.O., et al.: Application of aluminum nitride nanotubes as a promising nanocarriers for anticancer drug 5-aminosalicylic acid in drug delivery system. *J. Mol. Liq.* 352, 118676 (2022). <https://doi.org/10.1016/j.molliq.2022.118676> b) Jalili Sadrabad, M., Behrad, S., Sohanian, S.: Squamous cell carcinoma of the tongue, the importance of early diagnosis in danger zone: a case report. *Int. J. Sci. Res. Dent. Med. Sci.* 2, 63–66 (2020) c) Kazemi Rad, N., et al.: Incidence and risk factors of retinopathy of prematurity in Khatam Al-Anbia Ophthalmology Hospital in Mashhad City. *Int. J. Sci. Res. Dent. Med. Sci.* 1, 36–39 (2019)
45. Gowhari Shabgah, A., et al.: Does CCL 19 act as a double-edged sword in cancer development? *Clin. Exp. Immunol.* 207(2), 164–175 (2021). <https://doi.org/10.1093/cei/uxab039>
46. Mahawar, R., et al.: Nasal cavity malignant solitary fibrous tumor: a case report. *Int. J. Sci. Res. Dent. Med. Sci.* 4, 42–44 (2022)
47. Solano, N., et al.: A rare pleomorphic adenoma in an uncommon area: a case report. *Int. J. Sci. Res. Dent. Med. Sci.* 2, 59–62 (2020)
48. a) Marofi, F., et al.: Novel CAR T therapy is a ray of hope in the treatment of seriously ill AML patients. *Stem Cell Res. Ther.* 12(1), 465 (2021). <https://doi.org/10.1186/s13287-021-02420-8> b) Vakili-Samiani, S., et al.: Targeting Wee1 kinase as a therapeutic approach in hematological malignancies. *DNA Repair* 107, 103203 (2021). <https://doi.org/10.1016/j.dnarep.2021.103203> c) Marofi, F., et al.: CAR-NK cell in cancer immunotherapy; a promising frontier. *Cancer Sci.* 112(9), 3427–3436 (2021). <https://doi.org/10.1111/cas.14993>
49. Neshastehriz, A., et al.: Gold-coated iron oxide nanoparticles trigger apoptosis in the process of thermo-radiotherapy of U87-MG human glioma cells. *Radiat. Environ. Biophys.* 57(4), 405–418 (2018). <https://doi.org/10.1007/s00411-018-0754-5>
50. a) Honarvari, B., et al.: Folate-targeted curcumin-loaded niosomes for site-specific delivery in breast cancer treatment: in silico and in vitro study. *Molecules* 27(14), 4634 (2022). <https://doi.org/10.3390/molecules27144634> b) Mohanta, Y.K., et al.: Bio-inspired synthesis of silver nanoparticles from leaf extracts of *Cleistanthus collinus* (Roxb.): its potential antibacterial and anticancer activities. *IET Nanobiotechnol.* 12(3), 343–348 (2018). <https://doi.org/10.1049/iet-nbt.2017.0203> c) Hou, Q., et al.: Role of nutrient-sensing receptor GPRC6A in regulating colonic group 3 innate lymphoid cells and inflamed mucosal healing. *J. Crohns Colitis* 16(8), 1293–1305 (2022). <https://doi.org/10.1093/ecco-jcc/jjac020>
51. a) Sonbol, H., et al.: Bioinspired synthesise of CuO nanoparticles using *Cylindrospermum stagnale* for antibacterial, anticancer and larvicidal applications. *Appl. Nanosci.*, 1–11 (2021) b) Isaacfranklin, M., et al.: Single-phase Cr₂O₃ nanoparticles for biomedical applications. *Ceram. Int.* 46(12), 19890–19895 (2020). <https://doi.org/10.1016/j.ceramint.2020.05.050> c) Saravanan, M., et al.: Green synthesis of anisotropic zinc oxide nanoparticles with antibacterial and cytofriendly properties. *Microb. Pathog.* 115, 57–63 (2018). <https://doi.org/10.1016/j.micpath.2017.12.039>
52. a) Al-Enazi, N.M., et al.: Tin oxide nanoparticles (SnO₂-NPs) synthesis using *Galaxaura elongata* and its anti-microbial and cytotoxicity study: a greenery approach. *Appl. Nanosci.*, 1–9 (2021) b) Isaacfranklin, M., et al.: Y₂O₃ nanorods for cytotoxicity evaluation. *Ceram. Int.* 46(12), 20553–20557 (2020). <https://doi.org/10.1016/j.ceramint.2020.05.172>
53. a) Sonbol, H., et al.: Padina boryana mediated green synthesis of crystalline palladium nanoparticles as potential nanodrug against multidrug resistant bacteria and cancer cells. *Sci. Rep.* 11, 1–19 (2021) b) Vidhya, M.S., et al.: Anti-cancer applications of Zr, Co, Ni-doped ZnO thin nanoplates. *Mater. Lett.* 283, 128760 (2021). <https://doi.org/10.1016/j.matlet.2020.128760> c) Widjaja, G., et al.: Effect of tomato consumption on inflammatory markers in health and disease status: a systematic review and meta-analysis of clinical trials. *Clin. Nutr. ESPEN* 50, 93–100 (2022). <https://doi.org/10.1016/j.clnut.2022.03.001>

- doi.org/10.1016/j.chnesp.2022.04.019 d) Elveny, M., et al.: CFD-based simulation to reduce greenhouse gas emissions from industrial plants. *Int. J. Chem. React. Eng.* 19(11), 1179–1186 (2021). <https://doi.org/10.1515/ijcre-2021-0063>
54. a) Jalil, A.T., et al.: Hematological and serological parameters for detection of COVID-19. *J. Microbiol. Biotechnol. Food Sci.* 11(4), e4229 (2022). <https://doi.org/10.55251/jmbfs.4229> b) Saleh, M.M., et al.: Evaluation of immunoglobulins, CD4/CD8 T lymphocyte ratio and interleukin-6 in COVID-19 patients. *Turkish J. Immunol.* 8(3), 129–134 (2020). <https://doi.org/10.25002/tji.2020.1347> c) Widjaja, G., et al.: Humoral immune mechanisms involved in protective and pathological immunity during COVID-19. *Hum. Immunol.* 82(10), 733–745 (2021). <https://doi.org/10.1016/j.humimm.2021.06.011> d) Jalil, A.T., et al.: Viral hepatitis in Dhi-Qar Province: demographics and hematological characteristics of patients. *Int. J. Pharmaceut. Res.* 12, 2081–2087 (2020) e) Hussein, H.K., et al.: Association of cord blood asprosin concentration with atherogenic lipid profile and anthropometric indices. *Diabetol. Metab. Syndrome* 14, 1–6 (2022) f) Xu, Y., et al.: Prediction of COVID-19 manipulation by selective ACE inhibitory compounds of *Potentilla reptant* root: in silico study and ADMET profile. *Arab. J. Chem.* 15(7), 103942 (2022). <https://doi.org/10.1016/j.arabjc.2022.103942>
55. a) Moghadasi, S., et al.: A paradigm shift in cell-free approach: the emerging role of MSCs-derived exosomes in regenerative medicine. *J. Transl. Med.* 19, 1–21 (2021) b) Rahbaran, M., et al.: Cloning and embryo splitting in mammals: brief history, methods, and achievements. *Stem Cell. Int.* 2021, 2347506–11 (2021). <https://doi.org/10.1155/2021/2347506> c) Jalil, A.T., et al.: Polymerase chain reaction technique for molecular detection of HPV16 infections among women with cervical cancer in Dhi-Qar Province. *Mater. Today Proc.* 17, 1–7 (2021) d) Hanan, Z.K., et al.: WITHDRAWN: detection of human genetic variation in VAC14 gene by ARMA-PCR technique and relation with typhoid fever infection in patients with gallbladder diseases in Thi-Qar province/Iraq. *Mater. Today Proc.* (2021). <https://doi.org/10.1016/j.matpr.2021.05.236> e) Widjaja, G., et al.: Mesenchymal stromal/stem cells and their exosomes application in the treatment of intervertebral disc disease: a promising frontier. *Int. Immunopharm.* 105, 108537 (2022). <https://doi.org/10.1016/j.intimp.2022.108537> f) Ghaffar, S., et al.: What is the influence of grape products on liver enzymes? A systematic review and meta-analysis of randomized controlled trials. *Compl. Ther. Med.* 69, 102845 (2022). <https://doi.org/10.1016/j.ctim.2022.102845>
56. a) Akter, F., et al.: Cocos nucifera endocarp extract exhibits anti-diabetic and antilipidemic activities in diabetic rat model. *Int. J. Sci. Res. Dent. Med. Sci.* 4(1), 8–15 (2022) b) Leisangthem, T., et al.: Analgesic activity of aqueous extract of solanum xanthocarpum berries (SXB) in animal models. *Int. J. Sci. Res. Dent. Med. Sci.* 3(4), 179–183 (2021)
57. a) Barani, M., et al.: Recent application of cobalt ferrite nanoparticles as a theranostic agent. *Mater. Today Chem.* 26, 101131 (2022). <https://doi.org/10.1016/j.mtchem.2022.101131> b) Barani, M., et al.: Simulation, in vitro, and in vivo cytotoxicity assessments of methotrexate-loaded pH-responsive nanocarriers. *Polymers* 13(18), 3153 (2021). <https://doi.org/10.3390/polym13183153> c) Sargazi, S., et al.: Recent trends in mesoporous silica nanoparticles of rode-like morphology for cancer theranostics: a review. *J. Mol. Struct.* 1261, 132922 (2022). <https://doi.org/10.1016/j.molstruc.2022.132922>
58. a) Sabouri, Z., et al.: Plant-based synthesis of cerium oxide nanoparticles using *Rheum turkestanicum* extract and evaluation of their cytotoxicity and photocatalytic properties. *Mater. Technol.* 37(8), 555–568 (2022). <https://doi.org/10.1080/10667857.2020.1863573> b) Rabiee, N., et al.: Diatoms with invaluable applications in nanotechnology, biotechnology, and biomedicine: recent advances. *ACS Biomater. Sci. Eng.* 7, 3053–3068 (2021). <https://doi.org/10.1021/acsbomaterials.1c00475>
59. a) Jadoun, S., et al.: Synthesis of nanoparticles using microorganisms and their applications: a review. *Environ. Chem. Lett.* 20(5), 1–45 (2022). <https://doi.org/10.1007/s10311-022-01444-7> b) Hamidian, K., et al.: Cytotoxic performance of green synthesised Ag and Mg dual doped ZnO NPs using *Salvadora persica* extract against MDA-MB-231 and MCF-10 cells. *Arab. J. Chem.* 15(5), 103792 (2022). <https://doi.org/10.1016/j.arabjc.2022.103792> c) Cao, Y., et al.: Ceramic magnetic ferrite nanoribbons: eco-friendly synthesis and their antifungal and parasitocidal activity. *Ceram. Int.* 48(3), 3448–3454 (2022). <https://doi.org/10.1016/j.ceramint.2021.10.121>
60. Krishnamurthy, S., et al.: Dye-sensitized solar cells: fundamentals and current status. *Nanoscale Res. Lett.* 9, 1–9 (2014). <https://doi.org/10.1186/s11671-018-2760-6>
61. Zhang, J., et al.: Laser-assisted synthesis of superparamagnetic Fe@Au core-shell nanoparticles. *J. Phys. Chem. B* 110(14), 7122–7128 (2006). <https://doi.org/10.1021/jp0560967>
62. Petryk, A., et al.: Energy-based Treatment of Tissue and Assessment V, pp. 227–233. SPIE, San Jose (2009)
63. Chen, C.-C., et al.: Presence of gold nanoparticles in cells associated with the cell-killing effect of modulated electro-hyperthermia. *ACS Appl. Bio Mater.* 2(8), 3573–3581 (2019). <https://doi.org/10.1021/acsbm.9b00453>
64. Ogden, J., et al.: Energy-based Treatment of Tissue and Assessment V, pp. 200–210. SPIE, San Jose (2009)

How to cite this article: M. Alahdal, H., et al.: Trace elements-based Auroshell gold@hematite nanostructure: green synthesis and their hyperthermia therapy. *IET Nanobiotechnol.* 17(1), 22–31 (2023). <https://doi.org/10.1049/nbt2.12107>